

List of Supplementary Information

Affinity-based proteomics reveal cancer-specific networks coordinated by Hsp90

Kamalika Moulick^{1,†}, James H. Ahn^{1,†}, Hongliang Zong^{2,†}, Anna Rodina¹, Leandro Cerchietti², Erica M. Gomes DaGama¹, Eloisi Caldas-Lopes¹, Kristin Beebe³, Fabiana Perna¹, Katerina Hatzi², Ly P. Vu¹, Xinyang Zhao¹, Danuta Zatorska¹, Tony Taldone¹, Peter Smith-Jones⁴, Mary Alpaugh¹, Steven S. Gross⁵, Nagavarakishore Pillarsetty⁴, Thomas Ku⁴, Jason S. Lewis⁴, Steven M. Larson⁴, Ross Levine⁶, Hediye Erdjument-Bromage⁷, Monica L. Guzman², Stephen D. Nimer¹, Ari Melnick², Len Neckers³, Gabriela Chiosis¹

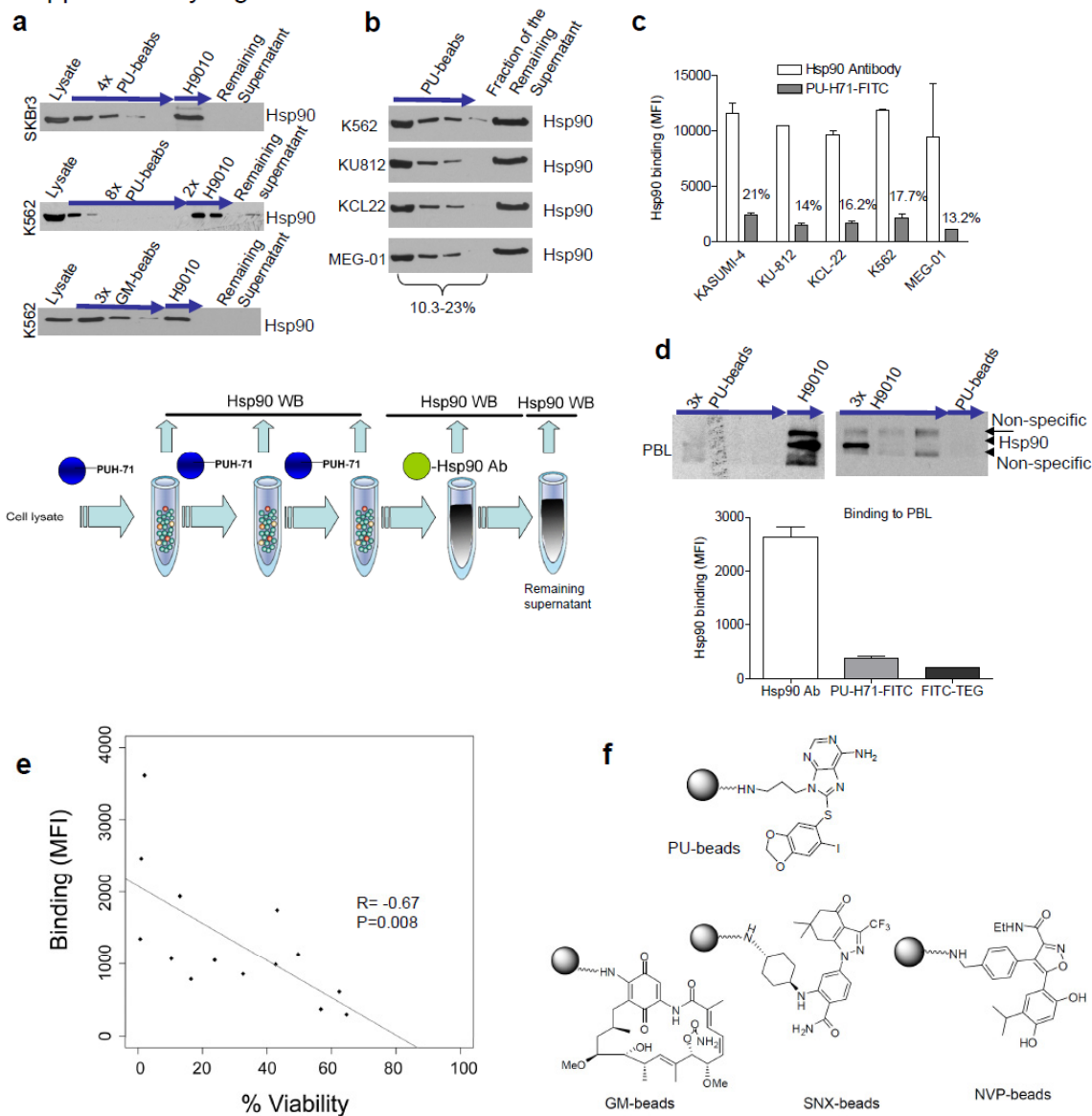
1. Molecular Pharmacology and Chemistry Program, Sloan-Kettering Institute, New York, NY
2. Division of Hematology and Oncology, Weill Cornell Medical College, New York, NY
3. Urologic Oncology Branch, Center for Cancer Research, National Cancer Institute, Bethesda, MD
4. Department of Radiology, Memorial Sloan-Kettering Cancer Center, New York, NY
5. Department of Pharmacology, Weill Medical College of Cornell University, New York, NY
6. Human Oncology and Pathogenesis Program and Leukemia Service, Department of Medicine, Memorial Sloan-Kettering Cancer Center, New York, NY
7. Microchemistry and Proteomics Core, Molecular Biology Program, Memorial Sloan-Kettering Cancer Center, New York, NY

Supplementary Results: Supplementary Figures 1 through 8

Supplementary Methods

Supplementary References

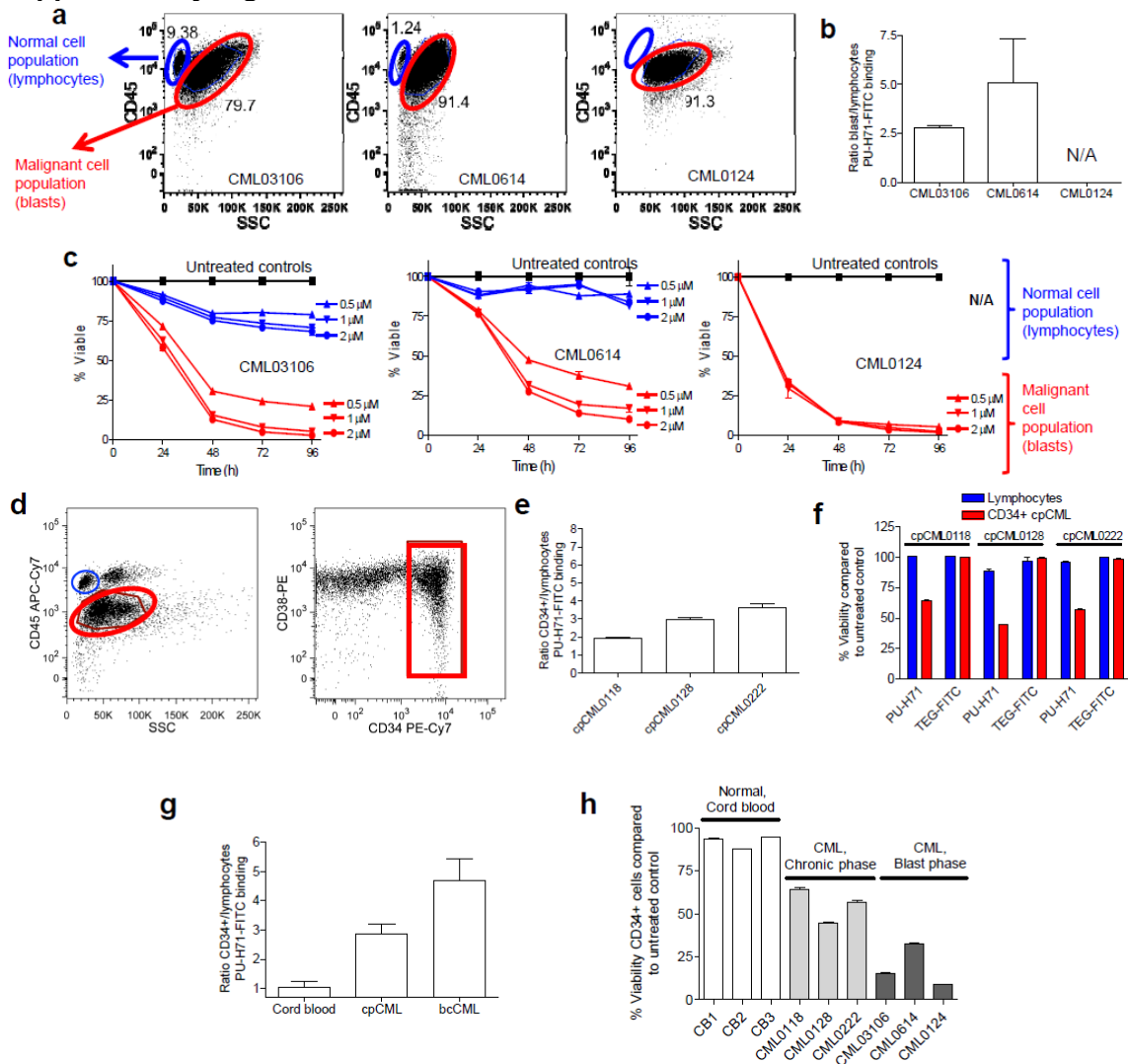
Supplementary Figure 1



Supplementary Figure 1. PU-H71 interacts with a restricted fraction of Hsp90 that is more abundant in cancer cells. **(a,b)** Hsp90 from breast cancer and CML cell extracts (120 μ g) was isolated through serial chemical- and immuno-purification steps, as indicated. The supernatant was isolated to analyze the left-over Hsp90. Hsp90 in each fraction was analyzed by Western blot. Lysate = endogenous protein content; PU-, GM- and Control-beads indicate proteins isolated on the particular beads. H9010 and IgG indicate protein isolated by the particular Ab. Control beads contain an Hsp90 inert molecule, 2-methoxyethylamine. The data are consistent with those obtained from multiple repeat experiments ($n \geq 2$). The lower panel shows schematically the sequential depletion methodology. **(c)** Hsp90 binding of PE conjugated antibody vs PU-H71-FITC. The percent of total cellular Hsp90 isolated by PU-H71 is indicated for each cell line above the data bar ($n=3$). **(d)** Sequential chemical- and immuno-purification steps were performed in peripheral blood leukocyte (PBL) extracts (250 μ g) to isolate PU-H71 and

H9010-specific Hsp90 species. All samples were analyzed by Western blot. (*upper*). Binding to Hsp90 in PBL was evaluated by flow cytometry using an Hsp90-PE antibody and PU-H71-FITC. FITC-TEG = control for non-specific binding (*lower*). (**e**) Correlation for binding of PU-H71-FITC (1 μ M) to Hsp90 versus percent viability after treatment with PU-H71 in a panel of 14 leukemia cell lines: Kasumi-1, Kasumi-4, KCL-22, REH, TF-1, KG-1, HL-60, OCI-AML3, K562, MOLM-13, TUR, THP-1, U937 and MV4-11. Total Hsp90 levels in these cells are similar, as demonstrated by Western blot (not shown). (**f**) Schematic representation of the solid-support immobilized Hsp90 inhibitors.

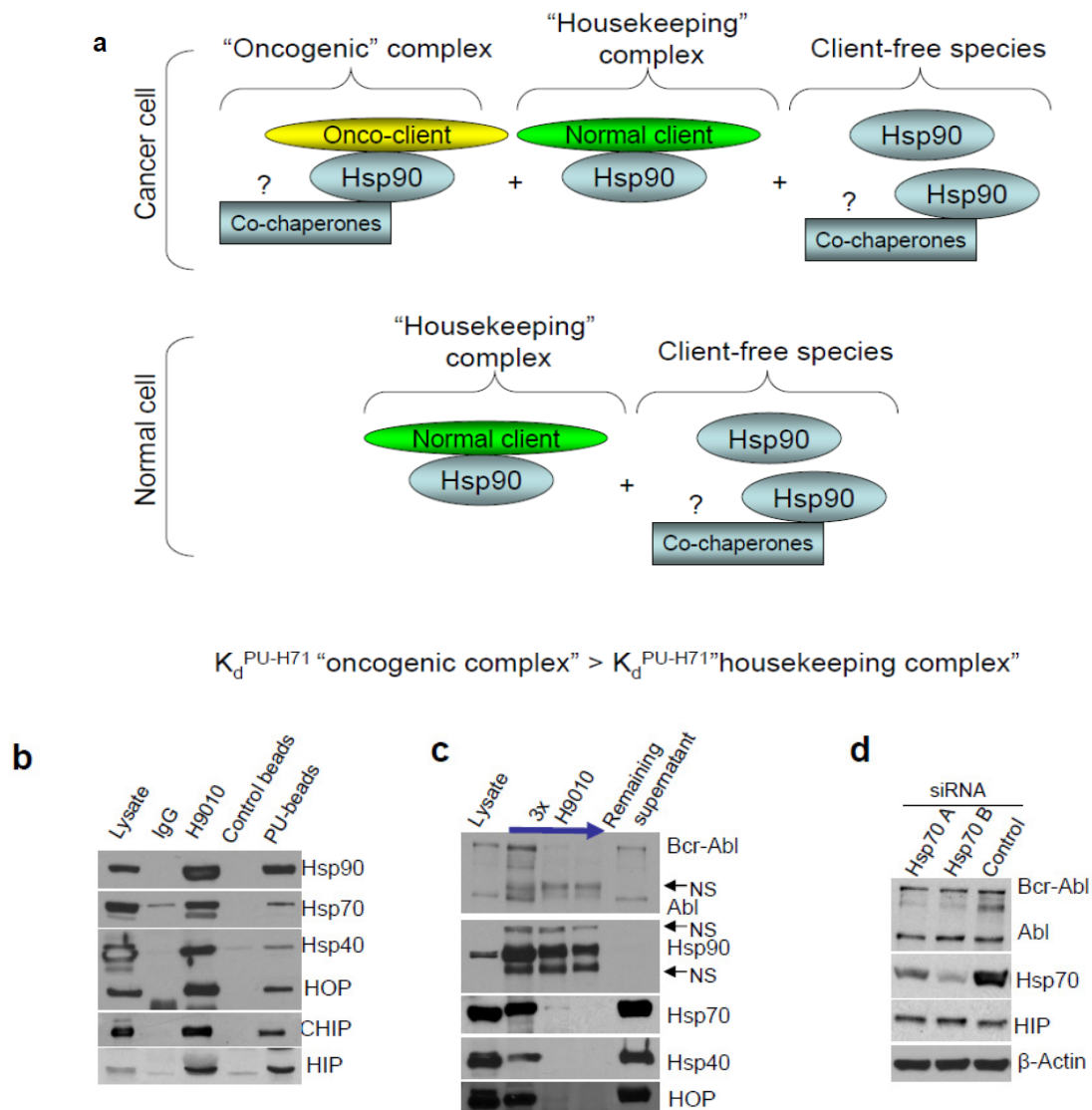
Supplementary Figure 2



Supplementary Figure 2. Cells with highest avidity for PU-H71 are also most sensitive to killing by the agent. (**a**) Flow cytometric dot plots demonstrate the gating strategy used for primary chronic myeloid leukemia (CML) samples to distinguish blast (CD45dim, red circles) and non-malignant lymphocytes (blue circles). (**b**) Ratio for PU-H71-FITC binding to Hsp90 in CML blasts to normal lymphocytes from the primary CML patient samples shown in (**a**). (**c**) Percent viability of CML blasts (red) or normal lymphocytes (blue) relative to untreated control for the primary CML samples shown in (**a**) after treatment at the indicated time points and doses of PU-H71. (**d**) Flow cytometric dot

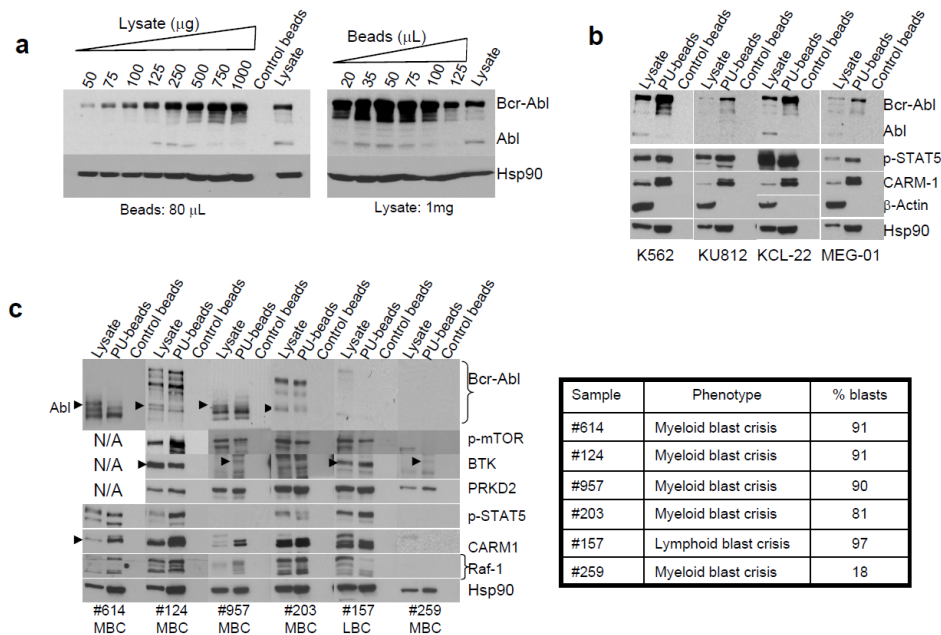
plots demonstrate the gating strategy used for primary chronic phase CML (cpCML) samples to distinguish blast (CD45dim, red circle) and non-malignant lymphocytes (blue circle) and to analyze binding of CD34+ cells (red square) within the blast gate (CD45dim, red circle). CD45 vs. SSC dot plots were pre-gated on viable cells based on 7-AAD discrimination. **(e)** Ratio for PU-H71-FITC binding to Hsp90 in chronic phase CML (cpCML) CD34+ cells and to normal lymphocytes. **(f)** Percent viability of cpCML CD34+ cells (red) and normal lymphocytes (blue) relative to untreated control after treatment for 48h with 1 μ M PU-H71-FITC or TEG-FITC. **(g)** Ratio for PU-H71-FITC binding to Hsp90 in CD34+ cells and lymphocytes from normal cord blood, chronic phase CML (cpCML) and blast phase (bpCML) cells (n=5). **(h)** Percent viability after 48h treatment with PU-H71 (1 μ M) of blast and chronic CML CD34+ cells, and normal CD34+ cells (from cord blood; CB) relative to untreated control. Cell viability in panels **c**, **f**, and **h** was evaluated by annexin V/7-AAD staining. Data are presented as means \pm SE (n = 3).

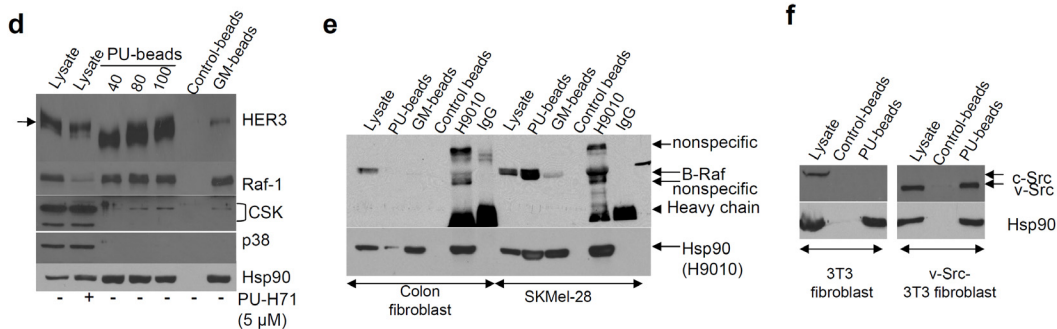
Supplementary Figure 3



Supplementary Figure 3. Cancer cells, unlike normal cells, harbor distinct pools of Hsp90 bound to either onco- or normal-client proteins. **(a)** Within normal cells, constitutive expression of Hsp90 is required for its evolutionarily conserved housekeeping function of folding and translocating cellular proteins to their proper cellular compartment (“housekeeping complex”). Upon malignant transformation, cellular proteins are perturbed through mutations, hyperactivity, retention in incorrect cellular compartments or other means. The presence of these functionally altered proteins is required to initiate and maintain the malignant phenotype, and it is these oncogenic proteins that are specifically maintained by a subset of stress modified Hsp90 (“oncogenic complex”). PU-H71 specifically binds to the fraction of Hsp90 that chaperones oncogenic proteins (“oncogenic complex”). **(b)** Hsp90 and its interacting co-chaperones were isolated in K562 cell extracts using PU- and Control-beads, and H9010 and IgG-immobilized Abs. Control beads contain an Hsp90 inert molecule, 2-methoxyethylamine. **(c)** Hsp90 from K562 cell extracts was isolated through three serial immuno-purification steps with the H9010 Hsp90 specific antibody. The remaining supernatant was isolated to analyze the left-over proteins. Proteins in each fraction were analyzed by Western blot. Lysate = endogenous protein content. The data are consistent with those obtained from multiple repeat experiments ($n \geq 2$). **(d)** Expression of proteins in Hsp70-knocked-down cells was analyzed by Western blot (*left*). Control = scramble siRNA.

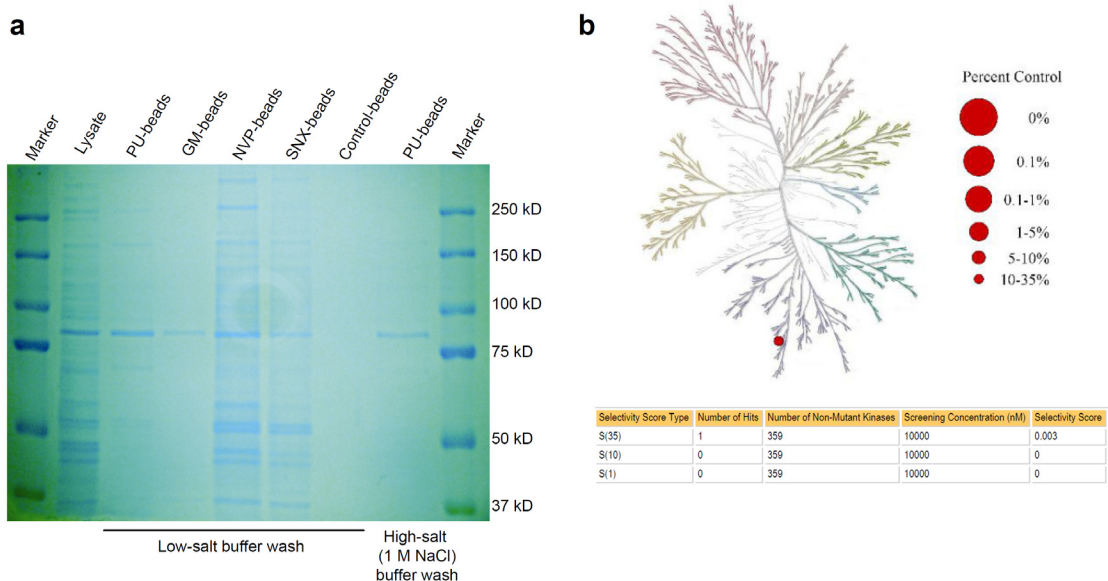
Supplementary Figure 4





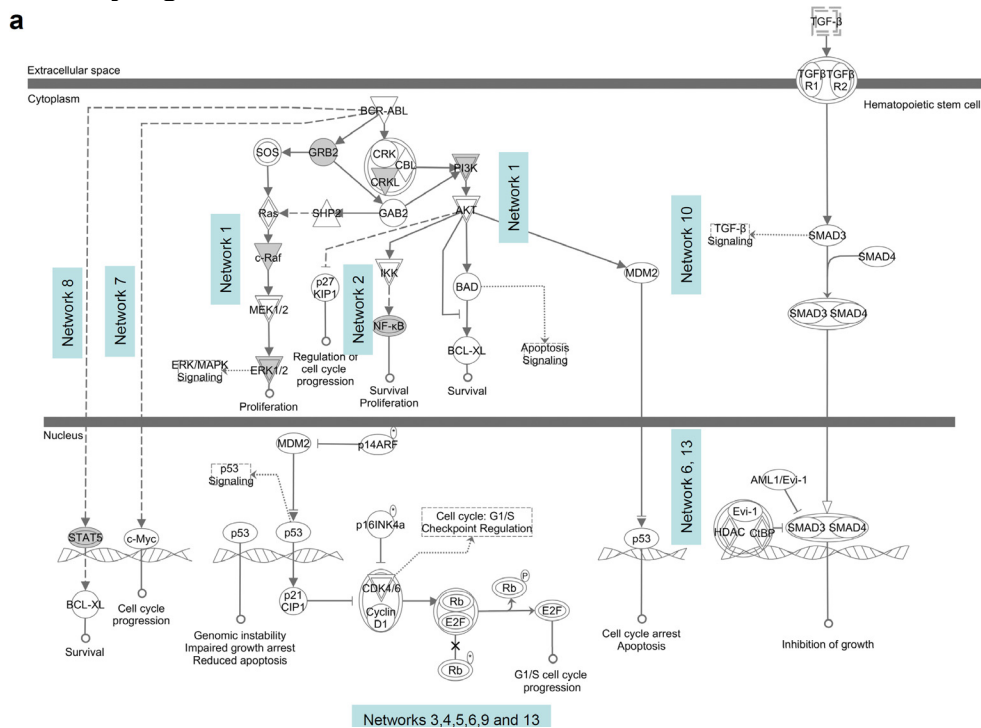
Supplementary Figure 4. GM and PU-H71 are selective for aberrant protein/Hsp90 species. (a) Bcr-Abl and Abl bound Hsp90 species were monitored in experiments where a constant volume of PU-H71 beads (80 μ L) was probed with indicated amounts of K562 cell lysate (*left*), or where a constant amount of lysate (1 mg) was probed with the indicated volumes of PU-H71 beads (*right*). (b,c) Single chemical-precipitations were conducted in Bcr-Abl-expressing CML cell lines (b) and in primary CML cell extracts (c) with PU- and Control-beads. Proteins in the pull-downs were analyzed by Western blot. Several Bcr-Abl cleavage products are noted in the primary CML samples as reported²². N/A = not available. (d) (*left*) PU- and GM-beads (80 μ L) recognize the Hsp90-mutant B-Raf complex in the SKMel28 melanoma cell extract (300 μ g), but fail to interact with the Hsp90-WT B-Raf complex found in the normal colon fibroblast CCD18Co extracts (300 μ g). H9010 Hsp90 Ab recognizes both Hsp90 species. (e) In MDA-MB-468 cell extracts (300 μ g), PU- and GM-beads (80 μ l) interact with HER3 and Raf-1 kinase but not with the non-oncogenic tyrosine-protein kinase CSK, a c-Src related tyrosine kinase, and p38. (f) (*right*) PU-beads (80 μ L) interact with v-Src/Hsp90 but not c-Src/Hsp90 species. To facilitate c-Src detection, a protein in lower abundance than v-Src, higher amounts of c-Src expressing 3T3 cell lysate (1,000 μ g) were used when compared to the v-Src transformed 3T3 cell (250 μ g), providing explanation for the higher Hsp90 levels detected in the 3T3 cells (Lysate, 3T3 fibroblasts vs v-Src 3T3 fibroblasts). Lysate = endogenous protein content; PU-, GM- and Control-beads indicate proteins isolated on the particular beads. Hsp90 Ab and IgG indicate protein isolated by the particular Ab. Control beads contain an Hsp90 inert molecule. The data are consistent with those obtained from multiple repeat experiments (n \geq 2).

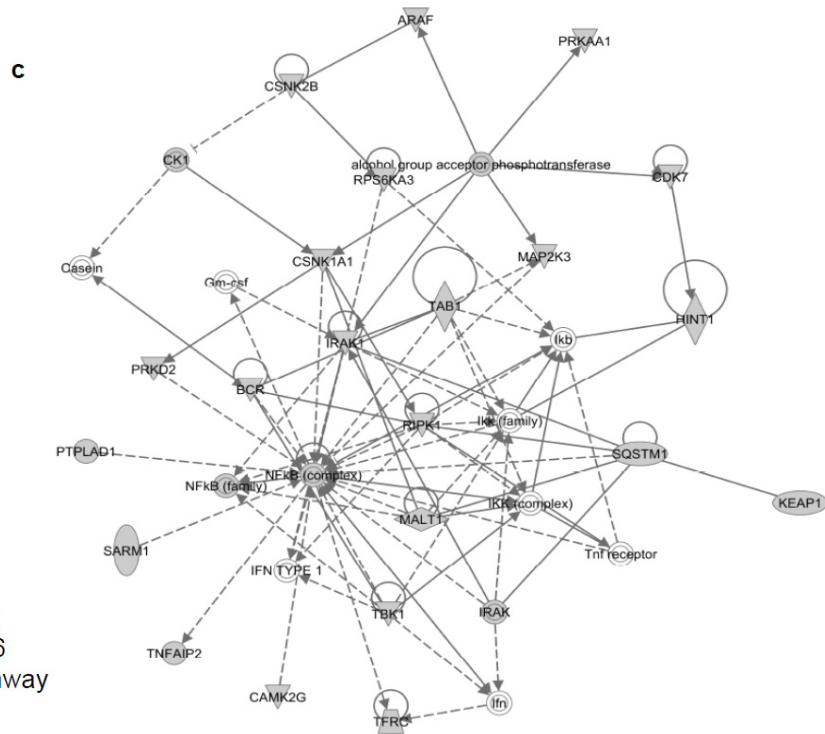
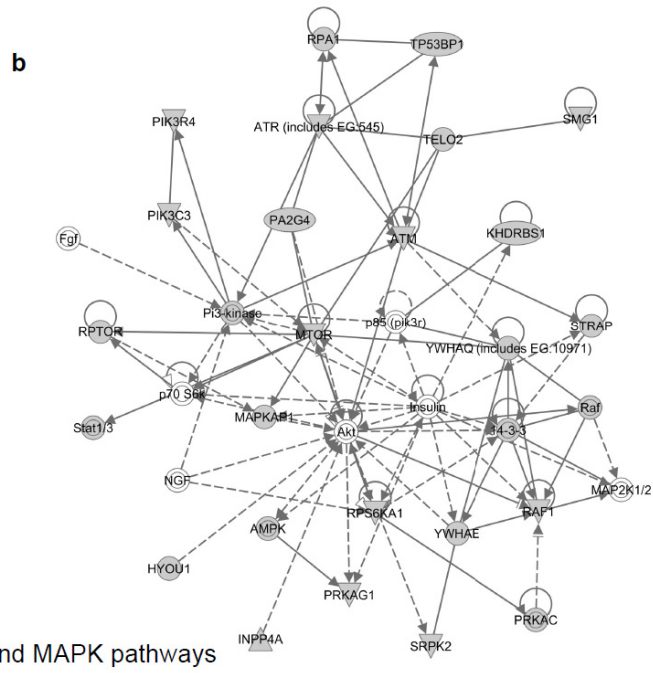
Supplementary Figure 5

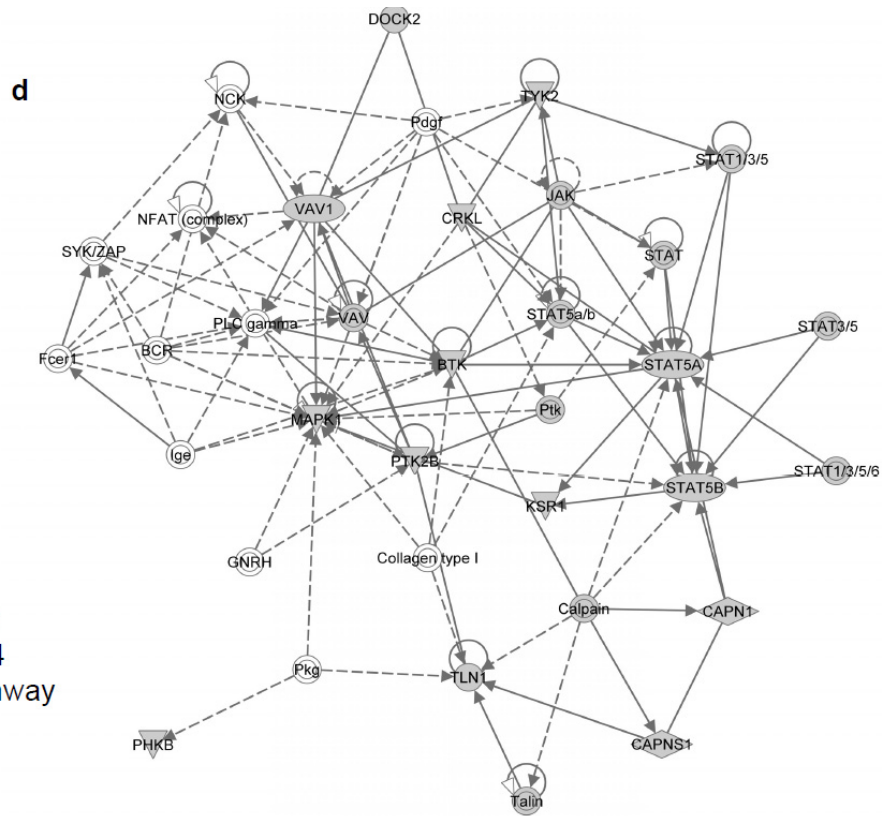


Supplementary Figure 5. PU-H71 is selective for Hsp90. **(a)** Coomassie stained gel of several Hsp90 inhibitor bead-pull-downs. K562 lysates (60 μ g) were incubated with 25 μ L of the indicated beads. Following washing with the indicated buffer, proteins in the pull-downs were applied to an SDS-PAGE gel. **(b)** PU-H71 (10 μ M) was tested in the scanMAX screen (Ambit) against 359 kinases. The TREEspot™ Interaction Map for PU-H71 is presented. Only SNARK (NUAK family SNF1-like kinase 2) (red dot on the kinase tree) appears as a potential low affinity kinase hit of the small molecule.

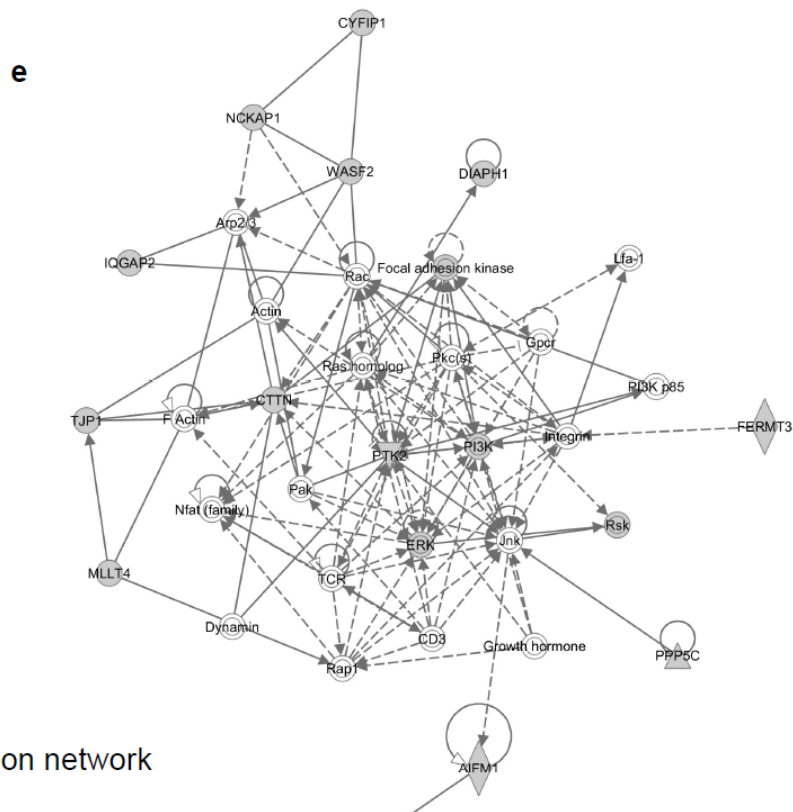
Supplementary Figure 6



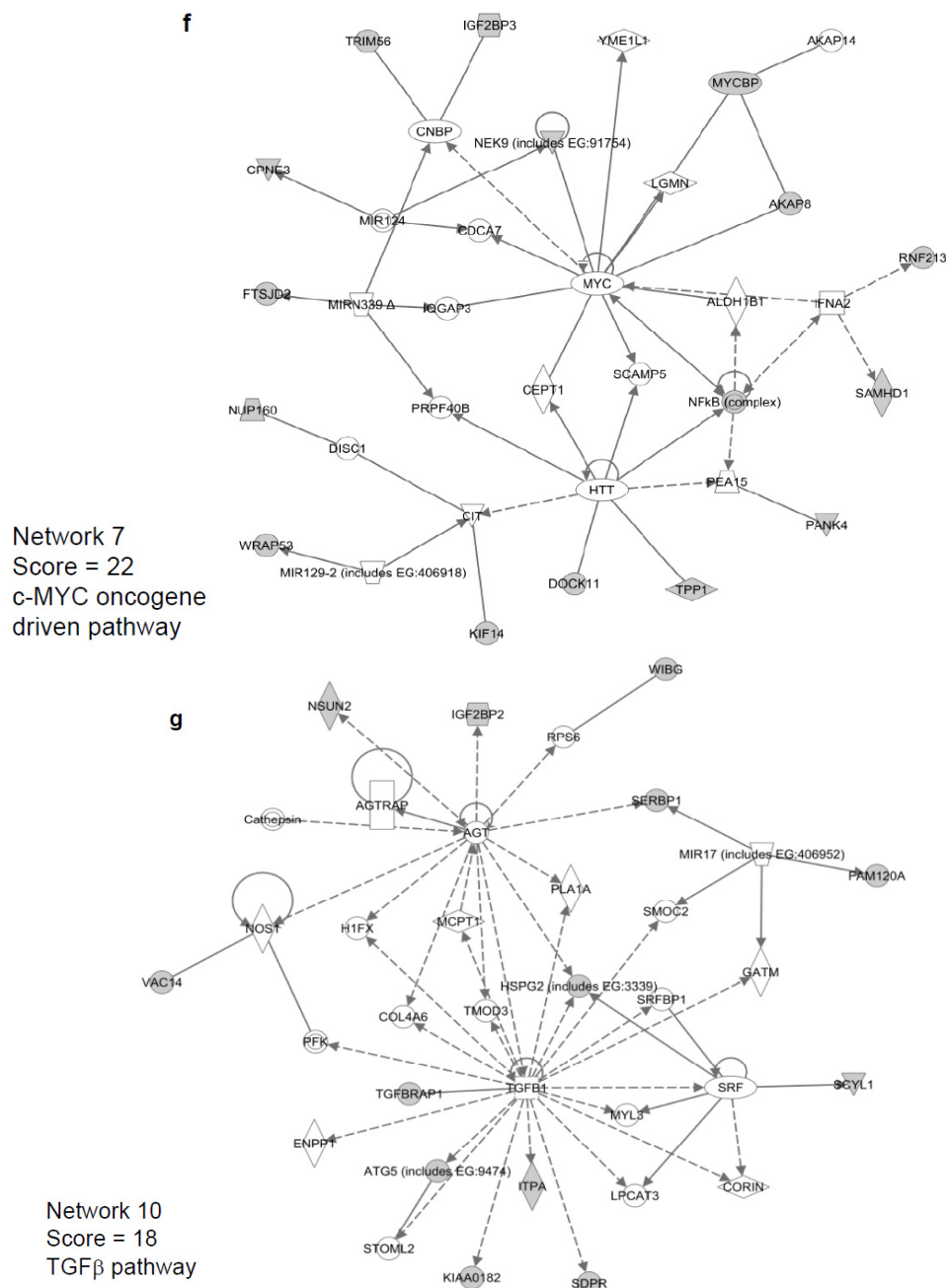




Network 8
Score = 14
STAT pathway



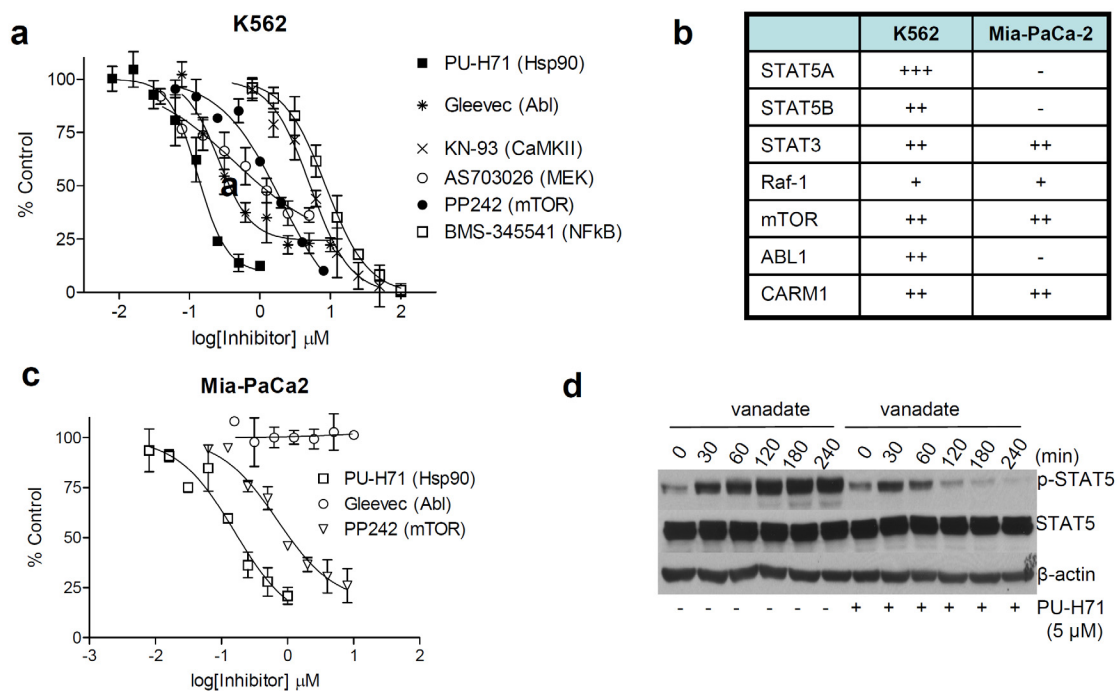
Network 12
Score = 13
Focal adhesion network



Supplementary Figure 6. Protein complexes were isolated through chemical precipitation by incubating a K562 extract with PU-beads, and the identity of proteins was probed by MS. Connectivity among these proteins was analyzed in IPA, and protein networks generated. (a) The protein networks identified by the PU-beads (Networks 1 through 13) overlap well with the known canonical myeloid leukemia signaling (provided by IPA). (b-g) Top scoring networks enriched on the PU-beads and as generated by bioinformatic pathways analysis through the use of the Ingenuity Pathways Analysis (IPA) software. (b) Network 1; Score = 38; mTOR/PI3K and MAPK pathways. (c) Network 2; Score = 36; NF κ B pathway. (d) Network 8; Score = 14; STAT pathway. (e) Network 12; Score = 13; Focal adhesion network. (f) Network 7; Score = 22; c-MYC

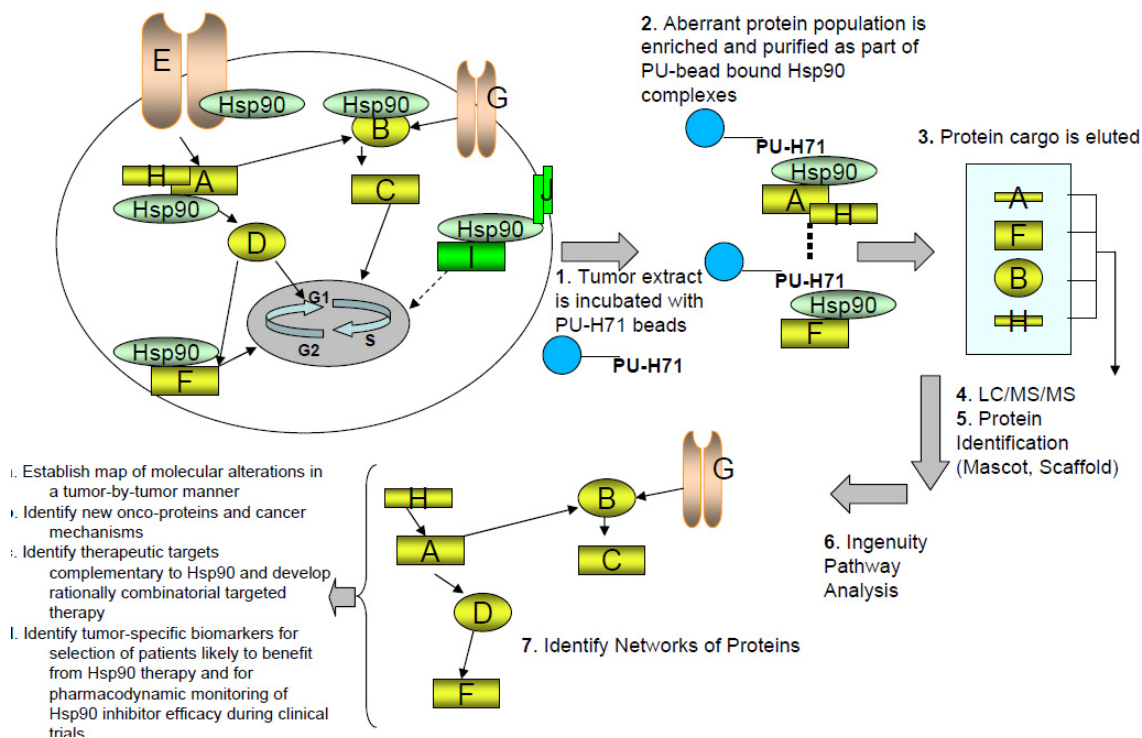
oncogene driven pathway. (g) Network 10; Score = 18; TGF β pathway. Scores of 2 or higher have at least a 99% confidence of not being generated by random chance alone. Gene expression, cell cycle and cellular assembly Individual proteins are displayed as nodes, utilizing gray to represent that the protein was identified in this study. Proteins identified by IPA only are represented as white nodes. Different shapes are used to represent the functional class of the gene product. Proteins are depicted in networks as two circles when the entity is part of a complex; as a single circle when only one unit is present; a triangle pointing up or down to describe a phosphatase or a kinase, respectively; by a horizontal oval to describe a transcription factor; and by circle to depict "other" functions. The edges describe the nature of the relationship between the nodes: an edge with arrow-head means that protein A *acts on* protein B, whereas an edge without an arrow-head represents binding only between two proteins. Direct interactions appear in the network diagram as a solid line, whereas indirect interactions as a dashed line. In some cases a relationship may exist as a circular arrow or line originating from one molecule and pointing back at that same molecule. Such relationships are termed "self-referential" and arise from the ability of a molecule to act upon itself.

Supplementary Figure 7



Supplementary Figure 7. PU-H71 cargo contributes to the malignant phenotype. **(a)** K562 cells were treated for 72h with the indicated inhibitors and cell growth analyzed by the Alamar Blue assay. Data are presented as means \pm SD ($n = 3$). **(b)** Select proteins isolated on PU-beads from K562 and Mia-PaCa-2 cell extracts, respectively, and subsequently identified by MS were tabulated. +++, very high; ++, high; +, moderate and -, no identifying peptides were found in MS analyses. **(c)** The effect of select inhibitors on Mia-PaCa-2 cell growth was analyzed as in panel **(a)**. **(d)** Representative Western blot of K562 cells treated for the indicated times with vanadate (1 mM) in the presence and absence of PU-H71 (5 μ M).

Supplementary Figure 8



Supplementary Figure 8. Schematic representation of the chemical-proteomics method for surveying tumor oncoproteins. Hsp90 forms biochemically distinct complexes in cancer cells. A major fraction of cancer cell Hsp90 retains “house keeping” chaperone functions similar to normal cells (green), whereas a functionally distinct Hsp90 pool enriched or expanded in cancer cells specifically interacts with oncogenic proteins required to maintain tumor cell survival (yellow). PU-H71 specifically interacts with Hsp90 and preferentially selects for onco-protein (yellow)/Hsp90 species but not WT protein (green)/Hsp90 species, and traps Hsp90 in a client binding conformation. The PU-H71 beads therefore can be used to isolate the onco-protein/Hsp90 species. In an initial step, the cancer cell extract is incubated with the PU-H71 beads (1). This initial chemical precipitation step purifies and enriches the aberrant protein population as part of PU-bead bound Hsp90 complexes (2). Protein cargo from PU-bead pull-downs is then eluted in SDS buffer, submitted to standard SDS-PAGE (3), and then the separated proteins are extracted and trypsinized for LC/MS/MS analyses (4). Initial protein identification is performed using the Mascot search engine, and is further evaluated using Scaffold Proteome Software (5). Ingenuity Pathway Analysis (IPA) is then used to build biological networks from the identified proteins (6,7). The created protein network map provides an invaluable template to develop personalized therapies that are optimally effective for a specific tumor.

Supplementary Materials and Methods

Reagents: The Hsp90 inhibitors, PU-H71¹, NVP-AUY922², SNX-2112^{3,4}, the solid-support immobilized⁴ and the fluorescein labeled⁵ derivatives were synthesized as previously reported. The synthesized compounds were fully characterized and structures confirmed by direct comparison to previous reports and determined to have a purity of >98%. We purchased Gleevec (>99%) from LC Laboratories, AS703026 (>99%) from Selleck, KN-93 from Tocris (>98%), and PP242 (≥98%), BMS-345541 (≥98%) and sodium vanadate from Sigma. All compounds were used as DMSO stocks.

Western Blotting: Cells were either treated with PU-H71 or DMSO (vehicle) for 24 h and lysed in 50 mM Tris, pH 7.4, 150 mM NaCl and 1% NP40 lysis buffer supplemented with leupeptin (Sigma Aldrich) and aprotinin (Sigma Aldrich). Protein concentrations were determined using BCA kit (Pierce) according to the manufacturer's instructions. Protein lysates (15-200 µg) were electrophoretically resolved by SDS/PAGE, transferred to nitrocellulose membrane and probed with the following primary antibodies against: Hsp90 (1:2000, SMC-107A/B; StressMarq), Bcr-Abl (1:75, 554148; BD Pharmingen), PI3K (1:1000, 06-195; Upstate), mTOR (1:200, Sc-1549; Santa Cruz), p-mTOR (1:1000, 2971; Cell Signaling), STAT3 (1:1000, 9132; Cell Signaling), p-STAT3 (1:2000, 9145; Cell Signaling), STAT5 (1:500, Sc-835; Santa Cruz), p-STAT5 (1:1000, 9351; Cell Signaling), RICTOR (1:2000, NB100-611; Novus Biologicals), RAPTOR (1:1000, 2280; Cell Signaling), P90RSK (1:1000, 9347; Cell Signaling), Raf-1 (1:300, Sc-133; Santa Cruz), CARM1 (1:1000, 09-818; Millipore), CRKL (1:200, Sc-319; Santa Cruz), GRB2 (1:1000, 3972; Cell Signaling), FAK (1:1000, Sc-1688; Santa Cruz), BTK (1:1000, 3533; Cell Signaling), A-Raf (1:1000, 4432; Cell Signaling), PRKD2 (1:200, sc-100415, Santa Cruz), HCK (1:500, 06-833; Millipore), p-HCK (1:500, ab52203; Abcam) and β-actin (1:2000, A1978; Sigma). The membranes were then incubated with a 1:3000 dilution of a corresponding horseradish peroxidase conjugated secondary antibody. Detection was performed using the ECL-Enhanced Chemiluminescence Detection System (Amersham Biosciences) according to manufacturer's instructions.

Densitometry: Gels were scanned in Adobe Photoshop 7.0.1 and quantitative densitometric analysis was performed using Un-Scan-It 5.1 software (Silk Scientific).

Nano-LC-MS/MS. Lysates prepared as mentioned above were first pre-cleaned by incubation with control beads overnight at 4°C. Pre-cleaned K562 cell extract (1,000 µg) in 200 µl RNeasy lysis buffer was incubated with PU-H71 or control-beads (80 µl) for 24 h at 4°C. Beads were washed with lysis buffer, proteins eluted by boiling in 2% SDS, separated on a denaturing gel and Coomassie stained according to manufacturer's procedure (Biorad). Gel-resolved proteins from pull-downs were digested with trypsin, as described⁶. In-gel tryptic digests were subjected to a micro-clean-up procedure⁷ on 2 µL bed-volume of Poros 50 R2 (Applied Biosystems – 'AB') reversed-phase beads, packed in an Eppendorf gel-loading tip, and the eluant diluted with 0.1% formic acid (FA). Analyses of the batch purified pools were done using a QSTAR-Elite hybrid quadrupole time-of-flight mass spectrometer (QToF MS) (AB/MDS Sciex), equipped with a nano spray ion source. Peptide mixtures (in 20 µL) are loaded onto a trapping guard column (0.3x5-mm PepMap C18 100 cartridge from LC Packings) using an Eksigent nano MDLC system (Eksigent Technologies, Inc) at a flow rate of 20 µL/min. After washing, the flow was reversed through the guard column and the peptides eluted with a 5-45% MeCN gradient (in 0.1% FA) over 85 min at a flow rate of 200 nL/min, onto and over a

75-micron x 15-cm fused silica capillary PepMap C18 column (LC Packings); the eluant is directed to a 75-micron (with 10-micron orifice) fused silica nano-electrospray needle (New Objective). Electrospray ionization (ESI) needle voltage was set at about 1800 V. The mass analyzer is operated in automatic, data-dependent MS/MS acquisition mode, with the threshold set to 10 counts per second of doubly or triply charged precursor ions selected for fragmentation scans. Survey scans of 0.25 sec are recorded from 400 to 1800 amu; up to 3 MS/MS scans are then collected sequentially for the selected precursor ions, recording from 100 to 1800 amu. The collision energy is automatically adjusted in accordance with the m/z value of the precursor ions selected for MS/MS. Selected precursor ions are excluded from repeated selection for 60 sec after the end of the corresponding fragmentation duty cycle. Initial protein identifications from LC-MS/MS data was done using the Mascot search engine (Matrix Science, version 2.2.04; www.matrixscience.com) and the NCBI (National Library of Medicine, NIH – human taxonomy containing, 223,695 protein sequences) and IPI (International Protein Index, EBI, Hinxton, UK – human taxonomy, containing 83,947 protein sequences) databases. One missed tryptic cleavage site was allowed, precursor ion mass tolerance = 0.4Da fragment ion mass tolerance = 0.4 Da, protein modifications were allowed for Met-oxide, Cys-acrylamide and N-terminal acetylation. MudPit scoring was typically applied with 'require bold red' activated, and using significance threshold score $p < 0.05$. Unique peptide counts (or 'spectral counts') and percent sequence coverages for all identified proteins were exported to Scaffold Proteome Software (version 2_06_01, www.proteomesoftware.com) for further bioinformatic analysis (**Supplementary Dataset 1a**). Using output from Mascot, Scaffold validates, organizes, and interprets mass spectrometry data, allowing more easily to manage large amounts of data, to compare samples, and to search for protein modifications. Findings were validated in a second MS system, the Waters Xevo QToF MS instrument (**Supplementary Dataset 1d**). Potential unspecific interactors were identified and removed from further analyses as indicated⁸.

Bioinformatic pathways analysis: Proteins were analyzed further by bioinformatic pathways analysis (Ingenuity Pathway Analysis 8.7 [IPA]; Ingenuity Systems, Mountain View, CA, www.ingenuity.com)^{9,10}. IPA constructs hypothetical protein interaction clusters based on a regularly updated "Ingenuity Pathways Knowledge Base". The Ingenuity Pathways Knowledge Base is a very large curated database consisting of millions of individual relationships between proteins, culled from the biological literature. These relationships involve direct protein interactions including physical binding interactions, enzyme substrate relationships, and cis-trans relationships in translational control. The networks are displayed graphically as nodes (individual proteins) and edges (the biological relationships between the nodes). Lines that connect two molecules represent relationships. Thus any two molecules that bind, act upon one another, or that are involved with each other in any other manner would be considered to possess a relationship between them. Each relationship between molecules is created using scientific information contained in the Ingenuity Knowledge Base. Relationships are shown as lines or arrows between molecules. Arrows indicate the directionality of the relationship, such that an arrow from molecule A to B would indicate that molecule A acts upon B. Direct interactions appear in the network diagram as a solid line, whereas indirect interactions as a dashed line. In some cases a relationship may exist as a circular arrow or line originating from one molecule and pointing back at that same molecule. Such relationships are termed "self-referential" and arise from the ability of a molecule to act upon itself. In practice, the dataset containing the UniProtKB identifiers of differentially expressed proteins is uploaded into IPA. IPA then builds hypothetical

networks from these proteins and other proteins from the database that are needed fill out a protein cluster. Network generation is optimized for inclusion of as many proteins from the inputted expression profile as possible, and aims for highly connected networks. Proteins are depicted in networks as two circles when the entity is part of a complex; as a single circle when only one unit is present; a triangle pointing up or down to describe a phosphatase or a kinase, respectively; by a horizontal oval to describe a transcription factor; and by circle to depict "other" functions. IPA computes a score for each possible network according to the fit of that network to the inputted proteins. The score is calculated as the negative base-10 logarithm of the p-value that indicates the likelihood of the inputted proteins in a given network being found together due to random chance. Therefore, scores of 2 or higher have at least a 99% confidence of not being generated by random chance alone. All the networks presented here were assigned a score of 10 or higher (**Supplementary Dataset 1f**).

Radioisotope binding studies and Hsp90 quantification studies: Saturation studies were performed with ^{131}I -PU-H71 and cells (K562, MDA-MB-468, SKBr3, LNCaP, DU-145, MRC-5 and PBL). Briefly, triplicate samples of cells were mixed with increasing amount of ^{131}I -PU-H71 either with or without 1 μM unlabeled PU-H71. The solutions were shaken in an orbital shaker and after 1 hr the cells were isolated and washed with ice cold Tris-buffered saline using a Brandel cell harvester. All the isolated cell samples were counted and the specific uptake of ^{131}I -PU-H71 determined. These data were plotted against the concentration of ^{131}I -PU-H71 to give a saturation binding curve. For the quantification of PU-bound Hsp90, 9.2×10^7 K562 cells, 6.55×10^7 KCL-22 cells, 2.55×10^7 KU182 cells and 7.8×10^7 MEG-01 cells were lysed to result in 6382, 3225, 1349 and 3414 μg of total protein, respectively. To calculate the percentage of Hsp90, cellular Hsp90 expression was quantified by using standard curves created of recombinant Hsp90 purified from HeLa cells (Stressgen#ADI-SPP-770).

Pulse-Chase. K562 cells were treated with Na_3VO_4 (1 mM) with or without PU-H71 (5 μM), as indicated. Cells were collected at indicated times and lysed in 50 mM Tris pH 7.4, 150 mM NaCl and 1% NP-40 lysis buffer, and were then subjected to western blotting procedure.

Tryptic digestion: K562 cells were treated for 30 min with vehicle or PU-H71 (50 μM). Cells were collected and lysed in 50 mM Tris pH 7.4, 150 mM NaCl, 1% NP-40 lysis buffer. STAT5 protein was immunoprecipitated from 500 μg of total protein lysate with an anti-STAT5 antibody (Santa Cruz, sc-835). Protein precipitates bound to protein G agarose beads were washed with trypsin buffer (50 mM Tris pH 8.0, 20 mM CaCl_2) and 33 ng of trypsin has been added to each sample. The samples were incubated at 37°C and aliquots were collected at the indicated time points. Protein aliquots were subjected to SDS-PAGE and blotted for STAT5.

Activated STAT5 DNA binding assay: The DNA-binding capacity of STAT5a and STAT5b was assayed by an ELISA-based assay (TransAM, Active Motif, Carlsbad, CA) following the manufacturer instructions. Briefly, 5×10^6 K562 cells were treated with PU-H71 1 and 10 μM or control for 24 h. Ten micrograms of cell lysates were added to wells containing pre-adsorbed STAT consensus oligonucleotides (5'-TTCCCGGAA-3'). For control treated cells the assay was performed in the absence or presence of 20 pmol of competitor oligonucleotides that contains either a wild-type or mutated STAT consensus binding site. Interferon-treated HeLa cells (5 μg per well) were used as positive controls for the assay. After incubation and washing, rabbit polyclonal anti-STAT5a or anti-

STAT5b antibodies (1:1000, Active Motif) was added to each well, followed by HRP-anti-rabbit secondary antibody (1:1000, Active Motif). After HRP substrate addition, absorbance was read at 450 nm with a reference wavelength of 655 nm (Synergy4, Biotek, Winooski, VT). In this assay the absorbance is directly proportional to the quantity of DNA-bound transcription factor present in the sample. Experiments were carried out in four replicates. Results were expressed as arbitrary units (AU) from the mean absorbance values with SEM.

Quantitative Chromatin Immunoprecipitation (Q-ChIP): Q-ChIP was made as previously described with modifications¹¹. Briefly, 10⁸ K562 cells were fixed with 1% formaldehyde, lysed and sonicated (Branson sonicator, Branson). STAT5 N20 (Santa Cruz) and Hsp90 (Zymed) antibodies were added to the pre-cleared sample and incubated overnight at 4 °C. Then, protein-A or G beads were added, and the sample was eluted from the beads followed by de-crosslinking. The DNA was purified using PCR purification columns (Qiagen). Quantification of the ChIP products was performed by quantitative PCR (Applied Biosystems 7900HT) using Fast SYBR Green (Applied Biosystems). Target genes containing STAT binding site were detected with the following primers: CCND2 (5-GTTGTTCTGGTCCCTTTAATCG and 5-ACCTCGCATACCCAGAGA), MYC (5-ATGCGTTGCTGGGTTATTTT and 5-CAGAGCGTGGGATGTTAGTG) and for the intergenic control region (5-CCACCTGAGTCTGCAATGAG and 5-CAGTCTCCAGCCTTTGTTCC).

Real time QPCR: RNA was extracted from PU-H71-treated and control K562 cells using RNeasy Plus kit (Qiagen) following the manufacturer instructions. cDNA was synthesized using High Capacity RNA-to-cDNA kit (Applied Biosystems). We amplified specific genes with the following primers: MYC (5-AGAAGAGCATCTTCCGCATC and 5-CCTTTAAACAGTGCCCAAGC), CCND2 (5-TGAGCTGCTGGCTAAGATCA and 5-ACGGTACTGCTGCAGGCTAT), BCL-XL (5-CTTTTGTGGA ACTCTATGGGAACA and 5-CAGCGGTTGAAGCGTTCCT), MCL1 (5-AGACCTTACGACGGGTTGG and 5-ACATTCCTGATGCCACCTTC), CCND1 (5-CCTGTCCTACTACCGCCTCA and 5-GGCTTCGATCTGCTCCTG), HPRT (5-CGTCTTGCTCGAGATGTGATG and 5-GCACACAGAGGGCTACAATGTG), GAPDH (5-CGACCACTTTGTCAAGCTCA and 5-CCCTGTTGCTGTAGCCAAAT), RPL13A (5-TGAGTGAAAGGGAGCCAGAAG and 5-CAGATGCCCCACTCACAAGA). Transcript abundance was detected using the Fast SYBR Green conditions (initial step of 20 sec at 95 °C followed by 40 cycles of 1 sec at 95 °C and 20 sec at 60 °C). The C_T value of the housekeeping gene (RPL13A) was subtracted from the correspondent genes of interest (ΔC_T). The standard deviation of the difference was calculated from the standard deviation of the C_T values (replicates). Then, the ΔC_T values of the PU-H71-treated cells were expressed relative to their respective control-treated cells using the $\Delta\Delta C_T$ method. The fold expression for each gene in cells treated with the drug relative to control treated cells is determined by the expression: $2^{-\Delta\Delta C_T}$. Results were represented as fold expression with the standard error of the mean for replicates.

Hsp70 knock-down. Transfections were carried out by electroporation (Amaxa) and the Nucleofector Solution V (Amaxa), according to manufacturer's instructions. Hsp70 knockdown studies were performed using siRNAs designed as previously reported¹² against the open reading frame of Hsp70 (HSPA1A; accession number NM_005345). Negative control cells were transfected with inverted control siRNA sequence (Hsp70C; Dharmacon RNA technologies). The active sequences against Hsp70 used for the study

are Hsp70A (5'-GGACGAGUUUGAGCACAAG-3') and Hsp70B (5'-CCAAGCAGACGCAGAUCUU-3'). Sequence for the control is Hsp70C (5'-GGACGAGUUGUAGCACAAG-3'). Three million cells in 2 mL media (RPMI supplemented with 1% L-glutamine, 1% penicillin and streptomycin) were transfected with 0.5 μ M siRNA according to the manufacturer's instructions. Transfected cells were maintained in 6-well plates and at 84h, lysed followed by standard Western blot procedures.

Kinase screen¹³. For most assays, kinase-tagged T7 phage strains were grown in parallel in 24-well blocks in an *E. coli* host derived from the BL21 strain. *E. coli* were grown to log-phase and infected with T7 phage from a frozen stock (multiplicity of infection = 0.4) and incubated with shaking at 32°C until lysis (90-150 min). The lysates were centrifuged (6,000 x g) and filtered (0.2 μ m) to remove cell debris. The remaining kinases were produced in HEK-293 cells and subsequently tagged with DNA for qPCR detection. Streptavidin-coated magnetic beads were treated with biotinylated small molecule ligands for 30 minutes at room temperature to generate affinity resins for kinase assays. The liganded beads were blocked with excess biotin and washed with blocking buffer (SeaBlock, Pierce), 1% BSA, 0.05 % Tween 20, 1 mM DTT) to remove unbound ligand and to reduce non-specific phage binding. Binding reactions were assembled by combining kinases, liganded affinity beads, and test compounds in 1x binding buffer (20 % SeaBlock, 0.17x PBS, 0.05 % Tween 20, 6 mM DTT). Test compounds were prepared as 40x stocks in 100% DMSO and directly diluted into the assay. All reactions were performed in polypropylene 384-well plates in a final volume of 0.04 ml. The assay plates were incubated at room temperature with shaking for 1 hour and the affinity beads were washed with wash buffer (1x PBS, 0.05 % Tween 20). The beads were then re-suspended in elution buffer (1x PBS, 0.05 % Tween 20, 0.5 μ m non-biotinylated affinity ligand) and incubated at room temperature with shaking for 30 minutes. The kinase concentration in the eluates was measured by qPCR. KINOMEscan's selectivity score (S) is a quantitative measure of compound selectivity. It is calculated by dividing the number of kinases that bind to the compound by the total number of distinct kinases tested, excluding mutant variants. TREEspot™ is a proprietary data visualization software tool developed by KINOMEscan¹³. Kinases found to bind are marked with red circles, where larger circles indicate higher-affinity binding. The kinase dendrogram was adapted and is reproduced with permission from Science and Cell Signaling Technology, Inc.

Lentiviral vectors, lentiviral production and K562 cells transduction. Lentiviral constructs of shRNA knock-down of CARM1 were purchased from the TRC lentiviral shRNA libraries of Openbiosystem: pLKO.1-shCARM1-KD1 (catalog No: RHS3979-9576107) and pLKO.1-shCARM1-KD2 (catalog No: RHS3979-9576108). The control shRNA (shRNA scramble) was Addgene plasmid 1864. GFP was cloned in to replace puromycin as the selection marker. Lentiviruses were produced by transient transfection of 293T as in the previously described protocol¹⁴. Viral supernatant was collected, filtered through a 0.45- μ m filter and concentrated. K562 cells were infected with high-titer lentiviral concentrated suspensions, in the presence of 8 μ g/ml polybrene (Aldrich). Transduced K562 cells were sorted for green fluorescence (GFP) after 72 hours transfection.

RNA extraction and quantitative Real-Time PCR (qRT-PCR). For qRT-PCR, total RNA was isolated from 10⁶ cells using the RNeasy mini kit (QIAGEN, Germany), and then subjected to reverse-transcription with random hexamers (SuperScript III kit,

Invitrogen). Real-time PCR reactions were performed using an ABI 7500 sequence detection system. The PCR products were detected using either Sybr green I chemistry or TaqMan methodology (PE Applied Biosystems, Norwalk, CT). Details for real-time PCR assays were described elsewhere¹⁵. The primer sequences for CARM1 qPCR are TGATGGCCAAGTCTGTCAAG(forward) and TGAAAGCAACGTCAAACCAG(reverse).

Cell viability, Apoptosis, and Proliferation assay. Viability assessment in K562 cells untransfected or transfected with CARM1 shRNA or scramble was performed using Trypan Blue. This chromophore is negatively charged and does not interact with the cell unless the membrane is damaged. Therefore, all the cells that exclude the dye are viable. Apoptosis analysis was assessed using fluorescence microscopy by mixing 2 μ L of acridine orange (100 μ g/mL), 2 μ L of ethidium bromide (100 μ g/mL), and 20 μ L of the cell suspension. A minimum of 200 cells was counted in at least five random fields. Live apoptotic cells were differentiated from dead apoptotic, necrotic, and normal cells by examining the changes in cellular morphology on the basis of distinctive nuclear and cytoplasmic fluorescence. Viable cells display intact plasma membrane (green color), whereas dead cells display damaged plasma membrane (orange color). An appearance of ultrastructural changes, including shrinkage, heterochromatin condensation, and nuclear degranulation, are more consistent with apoptosis and disrupted cytoplasmic membrane with necrosis. The percentage of apoptotic cells (apoptotic index) was calculated as: % Apoptotic cells = (total number of cells with apoptotic nuclei/total number of cells counted) x 100. For the proliferation assay, 5×10^3 K562 cells were plated on a 96-well solid black plate (Corning). The assay was performed according to the manufacturer's indications (CellTiter-Glo Luminescent Cell Viability Assay, Promega). All experiments were repeated three times. Where indicated, growth inhibition studies were performed using the Alamar blue assay. This reagent offers a rapid objective measure of cell viability in cell culture, and it uses the indicator dye resazurin to measure the metabolic capacity of cells, an indicator of cell viability. Briefly, exponentially growing cells were plated in microtiter plates (Corning # 3603) and incubated for the indicated times at 37 °C. Drugs were added in triplicates at the indicated concentrations, and the plate was incubated for 72 h. Resazurin (55 μ M) was added, and the plate read 6 h later using the Analyst GT (Fluorescence intensity mode, excitation 530nm, emission 580nm, with 560nm dichroic mirror). Results were analyzed using the Softmax Pro and the GraphPad Prism softwares. The percentage cell growth inhibition was calculated by comparing fluorescence readings obtained from treated versus control cells. The IC₅₀ was calculated as the drug concentration that inhibits cell growth by 50%.

Flow cytometry. *CD34 isolation* – CD34+ cell isolation was performed using CD34 MicroBead Kit and the automated magnetic cell sorter autoMACS according to the manufacturer's instructions (Miltenyi Biotech, Auburn, CA). *Viability assay* – CML cells lines were plated in 48-well plates at the density of 5×10^5 cells/ml, and treated with indicated doses of PU-H71. Cells were collected every 24 h, stained with Annexin V-V450 (BD Biosciences) and 7-AAD (Invitrogen) in Annexin V buffer (10 mM HEPES/NaOH, 0.14 M NaCl, 2.5 mM CaCl₂). Cell viability was analyzed by flow cytometry (BD Biosciences). For patient samples, primary blast crisis CML cells were plated in 48-well plates at 2×10^6 cells/ml, and treated with indicated doses of PU-H71 for up to 96 h. Cells were stained with CD34-APC, CD38-PE-CY7 and CD45-APC-H7 antibodies (BD Biosciences) in FACS buffer (PBS, 0.05% FBS) at 4 °C for 30 min prior to Annexin V/7-AAD staining. *PU-H71 binding assay* – CML cells lines were plated in 48-well plates at the density of 5×10^5 cells/ml, and treated with 1 μ M PU-H71-FITC. At 4 h

post treatment, cells were washed twice with FACS buffer. To measure PU-H71-FITC binding in live cells, cells were stained with 7-AAD in FACS buffer at room temperature for 10 min, and analyzed by flow cytometry (BD Biosciences). At 48h, and 96 h post PU-H71-FITC treatment, cells were stained with Annexin V-V450 (BD Biosciences) and 7-AAD in Annexin V buffer, and subjected to flow cytometry to measure viability determined by AnnexinV/7AAD double negative gates. To evaluate the binding of PU-H71-FITC to leukemia patient samples, primary bp or cpCML cells were plated in 48-well plates at 2×10^6 cells/ml, and treated with 1 μ M PU-H71-FITC. At 24 h post treatment, cells were washed twice, and stained with CD34-APC (or CD34-PECy7), CD38-PE-CY7 (or CD38-PE) and CD45-APC-H7 antibodies in FACS buffer at 4°C for 30 min prior to 7-AAD staining. At 48h, and 96 h post treatment, cells were stained with CD34-APC (or CD34-PECy7), CD38-PE-CY7 (or CD38-PE) and CD45-APC-H7 antibodies followed by Annexin V-V450 and 7-AAD staining to measure cell viability in blast, lymphocytes and CD34+ cell populations. For competition test, CML cell lines at the density of 5×10^5 cells/ml or primary CML samples at the density of 2×10^6 cells/ml were treated with 1 μ M unconjugated PU-H71 for 4 h followed by treatment of 1 μ M PU-H71-FITC for 1 h. Cells were collected, washed twice, stained for 7-AAD in FACS buffer, and analyzed by flow cytometry. *HSP90 staining* – Cells were fixed with fixation buffer (BD Biosciences) at 4°C for 30 min, and permeabilized in Perm Buffer III (BD Biosciences) on ice for 30 min. Cells were stained with anti-HSP90 phycoerythrin conjugate (PE) (F-8 clone, Santa Cruz Biotechnologies; CA) for 60 minutes. Cells were washed and then analyzed by flow cytometry. Normal mouse IgG2a-PE was used as isotype control.

Cell separation: CD45 vs SSC gating is commonly used to separate and distinguish different cell populations in normal and malignant hematopoiesis by flow cytometry¹⁶⁻¹⁹. Blast cells are often quantified and characterized by dim CD45 staining, in contrast to the circulating non-blast cell populations, which are CD45hi. In most studies, when the sorted cells are reanalyzed, both cell populations are > 95% pure²⁰. Thus, the use of the CD45lo/ SSC+ cells vs the CD45hi/ SSC- cells is appropriate to simultaneously examine the response of blast cells vs. normal lymphocytes to agents such as PU-H71. It is feasible that a small percent of lymphocytes carry the BCR-ABL translocation, and these cells will be represented within the CD45hi gate²¹. However, a small percent of BCR-ABL+ cells in the CD45hi population will not affect the results of the biochemical assays conducted here.

Supplementary References

1. He, H. *et al.* Identification of potent water soluble purine-scaffold inhibitors of the heat shock protein 90. *J. Med. Chem.* **49**, 381-390 (2006).
2. Brough, P. A. *et al.* 4,5-Diarylisoxazole hsp90 chaperone inhibitors: potential therapeutic agents for the treatment of cancer. *J. Med. Chem.* **51**, 196-218 (2008).
3. Huang, K. H. *et al.* Discovery of novel 2-aminobenzamide inhibitors of heat shock protein 90 as potent, selective and orally active antitumor agents. *J. Med. Chem.* **52**, 4288-4305 (2009).
4. Taldone, T. *et al.* Design, synthesis and evaluation of small molecule Hsp90 probes. *Bioorg. Med. Chem.* **19**, 2603–2614 (2011).
5. Taldone, T. *et al.* Synthesis of purine-scaffold fluorescent probes for heat shock protein 90 with use in flow cytometry and fluorescence microscopy. *Bioorg. Med. Chem. Lett.* (2011).

6. Winkler, G S. *et al.* Isolation and mass spectrometry of transcription factor complexes. *Methods* **26**, 260-269 (2002).
7. Erdjument-Bromage, H. *et al.* Micro-tip reversed-phase liquid chromatographic extraction of peptide pools for mass spectrometric analysis. *J. Chromatogr. A* **826**, 167-181 (1998).
8. Trinkle-Mulcahy, L., *et al.* Identifying specific protein interaction partners using quantitative mass spectrometry and bead proteomes. *J. Cell. Biol.* **183**, 223-239 (2008).
9. Munday, D. *et al.* Quantitative proteomic analysis of A549 cells infected with human respiratory syncytial virus. *Mol. Cell Proteomics* **9**, 2438-2459 (2010).
10. Andersen, J.N. *et al.* Pathway-Based Identification of Biomarkers for Targeted Therapeutics: Personalized Oncology with PI3K Pathway Inhibitors. *Sci. Transl. Med.* **2**, 43ra55 (2010).
11. Cerchietti, L.C. *et al.* A purine scaffold Hsp90 inhibitor destabilizes BCL-6 and has specific antitumor activity in BCL-6-dependent B cell lymphomas. *Nat. Med.* **15**, 1369-1376 (2009).
12. Powers, M.V., Clarke, P.A., Workman, P. Dual targeting of Hsc70 and Hsp72 inhibits Hsp90 function and induces tumor-specific apoptosis. *Cancer Cell* **14**, 250-262 (2008).
13. Fabian, M.A. *et al.* A small molecule-kinase interaction map for clinical kinase inhibitors. *Nat. Biotechnol.* **23**, 329-336 (2005).
14. Moffat, J. *et al.* A Lentiviral RNAi Library for Human and Mouse Genes Applied to an Arrayed Viral High-Content Screen. *Cell* **124**, 1283-1298 (2006).
15. Zhao, X. *et al.* Methylation of RUNX1 by PRMT1 abrogates SIN3A binding and potentiates its transcriptional activity. *Genes Dev.* **22**, 640-653 (2009).
16. Ratej, R. *et al.* Normal lymphocytes from leukemic samples as an internal quality control for fluorescence intensity in immunophenotyping of acute leukemias. European Working Group of Clinical Cell Analysis (EWGCCA). *Cytometry B Clin. Cytom.* **70**, 1-9 (2006).
17. Wood, B.L. Myeloid malignancies: myelodysplastic syndromes, myeloproliferative disorders, and acute myeloid leukemia. *Clin. Lab. Med.* **27**, 551-75 (2007).
18. Jennings, C.D. *et al.* Recent advances in flow cytometry: application to the diagnosis of hematologic malignancy. *Blood* **90**, 2863-2892 (1997).
19. Vial, J.P. & Lacombe, F. Immunophenotyping of acute leukemia: utility of CD45 for blast cell identification. *Methods Cell. Biol.* **64**, 343-58 (2001).
20. Tabrizi, R. *et al.* Resistance to daunorubicin-induced apoptosis is not completely reversed in CML blast cells by STI571. *Leukemia* **16**, 1154-1159 (2002).
21. Takahashi, N., Miura, I., Saitoh, K. & Miura, A.B. Lineage involvement of stem cells bearing the philadelphia chromosome in chronic myeloid leukemia in the chronic phase as shown by a combination of fluorescence-activated cell sorting and fluorescence in situ hybridization. *Blood* **92**, 4758-4763 (1998).
22. Dierov, J., Dierova, R. & Carroll, M. BCR/ABL translocates to the nucleus and disrupts an ATR-dependent intra-S phase checkpoint. *Cancer Cell* **5**, 275-85 (2004).